ROCKING DAMAGE-FREE STEEL COLUMN BASE WITH FRICTION DEVICES: DESIGN PROCEDURE AND GLOBAL SEISMIC RESPONSE OF BUILDINGS.

Fabio Freddi*,[a], Christoforos A. Dimopoulos[a], and Theodore L. Karavasilis[b]

[a] University of Warwick, School of Engineering, U.K.
F.Freddi@warwick.ac.uk, C.Dimopoulos@warwick.ac.uk
[b] University of Southampton, Faculty of Engineering and the Environment, U.K.
T.Karavasilis@soton.ac.uk

ABSTRACT

Resilient minimal-damage steel frames, such as post-tensioned self-centering steel frames or steel frames with passive dampers, have been extensively studied but little attention has been paid to their column bases. This paper presents a rocking damage-free steel column base using post-tensioned high strength steel bars to control rocking behavior and friction devices that provide stable energy dissipation capacity. Contrary to conventional steel column bases, the monotonic and cyclic hysteretic moment-rotation behavior of the proposed column base can be easily described using simple analytical equations. The paper describes in detail a step-by-step design procedure for the column base that ensures damage-free behavior and adequate self-centering and energy dissipation capacity. A finite element model for the column base is developed in OpenSees and used to conduct nonlinear dynamic (seismic) analyses of a building using self-centering steel moment-resisting frames. The results of the analyses show that the column base helps the building to avoid damage in the 1st story columns along with eliminating the 1st story residual drifts under both the design and maximum considered earthquake intensities.

Keywords: Column base; Steel frames; Seismic design; Resilience

1 INTRODUCTION

Conventional seismic-resistant structures, such as steel moment resisting frames (MRFs), are designed to experience significant inelastic deformations under strong earthquakes [1, 2]. Inelastic deformations result in damage of structural members and residual story drifts, which lead to high repair costs and disruption of the building use or occupation. The aforementioned socio-economic risks highlight the need for widespread implementation of minimal-damage structures, which can reduce both repair costs and downtime. Examples of such structures include steel frames equipped with self-centering beam-column connections, structural fuses, passive energy dissipation devices, self-centering braces, and others [3, 4]. These earthquake-resilient steel frame typologies have been extensively studied during the last decade but little attention has been paid to the behavior of their column bases.

Conventional steel column bases typically consist of an exposed steel base plate supported on grout and secured to the concrete foundation using steel anchor rods. In terms of their strength, column bases are typically designed as full-strength so that plastic hinges are developed in the bottom end of the first story columns [1, 5]. Apart from the fact that plastic hinges in the columns induce non-repairable damage, this design approach needs very strong column bases with adequate over-strength to account for material variability [6]. Alternatively, Eurocode 8 allows the design of partial-strength column bases, which are designed to develop plastic deformations [1, 5]. Such design philosophy however needs the knowledge of the plastic rotation capacity of the column base under cyclic loading, which is difficult to predict [7, 8]. Most importantly, field observations after strong earthquakes confirmed the susceptibility of column bases to difficult-to-repair damage such as concrete crushing, weld fracture, anchor rod fracture and base plate yielding [9].

Few research works proposed alternative column bases with the goal of overcoming the shortcomings of conventional column bases. Mackinven et al. [10] proposed a steel column base that involves the use of unbounded steel bars to act as re-centering devices while the column rocks under lateral loads. This column base lacks energy dissipation and develops significant stress concentration during rocking. MacRae et al. [11] proposed a steel column base where a pin is used to resist axial and shear forces. Flexural resistance and energy dissipation is provided by friction due to relative movement of the column flanges with respect to foundation flange plates with slotted holes. This column base has minimal-damage behavior in the strong column axis direction. Yamanishi et al. [12] developed a steel column base that involves exposed yield bolts anchored on a strong plate welded on the column and connected to the foundation anchor bolts through couplers. The yield bolts are the only components that experience damage and can be easily replaced. Chi and Liu [13] developed a damage-free steel column base that involves post-tensioned (PT) bars anchored at the mid-story height and at the bottom of a grade steel beam. Energy dissipation is provided by buckling-restrained steel plates, while shear resistance by bolted keeper plates. Chou and Chen [14] developed a similar self-centering column base but with PT bars anchored at the top and at the base of the first story columns. Recently, Borzouie et al. [15] presented experimental results on the behavior of a column base using an asymmetric friction connection. The system experiences rocking and energy is dissipated with friction/sliding surfaces parallel to the column strong axis. Superior behavior was achieved under loading in the column strong axis direction, while damage and stiffness degradation were observed under loading in the column weak axis direction.

This paper presents a rocking damage-free steel column base, which uses PT high strength steel bars to control rocking behavior and friction devices to dissipate seismic energy. Contrary to conventional steel column bases, the rocking column base has monotonic and cyclic moment-rotation behaviors that are easily described using simple analytical equations. Analytical equations are provided for different cases including structural limit states that involve yielding or loss of post-tensioning in the PT bars. A step-by-step design procedure is presented, which ensures damage-free behavior, self-centering capability, and adequate energy dissipation capacity for a predefined target column base rotation. The procedure provides optimum designs of the column base by using a simple graphical method. A finite element (FE) model for the column base is developed in OpenSees [16] and a prototype steel building is designed as a self-centering moment-resisting frame (SC-MRF) with conventional or rocking column bases. Nonlinear dynamic analyses show that the rocking column base fully protects the first story columns from yielding and eliminate the first story residual story drift without any detrimental effect on peak story drifts. More details can be found in Freddi et al. [17]. The latter study presents a three-dimensional nonlinear FE model for the column base in ABAQUS [18], which is used in order to validate the accuracy of the moment-rotation analytical equations and to demonstrate the efficiency of the design procedure.

2 ROCKING DAMAGE-FREE COLUMN BASE

2.1 Structural Details

Fig. 1(a) shows the proposed rocking damage-free column base, which in concept has similarities with the column base proposed by Kamperidis et al. [19]. A thick steel plate with rounded edges is welded on the bottom of a circular hollow steel section. The rounded edges help the column base to avoid stress concentration and damage during rocking of the hollow steel section on the steel base plate. Four PT high strength steel bars (or alternatively strands) are symmetrically placed around the center of the column base to increase the axial force and further control the rocking behavior. The PT bars are anchored to the bottom of the foundation (by running through steel ducts) and to a thick plate welded on the top of the hollow steel section (*i.e.* anchor plate in *Fig. 1(a)*). Friction devices (FDs) are placed to the four sides of the column base to provide energy dissipation during rocking. As shown in *Fig. 2(a)*, the FDs consist of two external steel plates bolted to the base plate; an internal steel plate welded to the circular hollow section; and two plates of brass material in the interface. Rocking of the column base results in sliding of the internal plate with respect to the brass

and external plates, and thus, in energy dissipation due to friction. The internal plate is drilled with inclined slotted holes to enable sliding, while the external plates and the brass plates are drilled with aligned rounded holes to accommodate four pre-tensioned bolts that are used to tune the friction force in the FDs. The dimensions of the inclined slotted holes are chosen to accommodate the superposition of all possible bolt travel paths during rocking of the column base as shown in *Fig. 2(a)*. As shown in *Fig. 2(b)*, a shear key is used to provide shear resistance to the column base. The shape of the shear key is designed with the goal of avoiding interlocking during rocking of the column base.

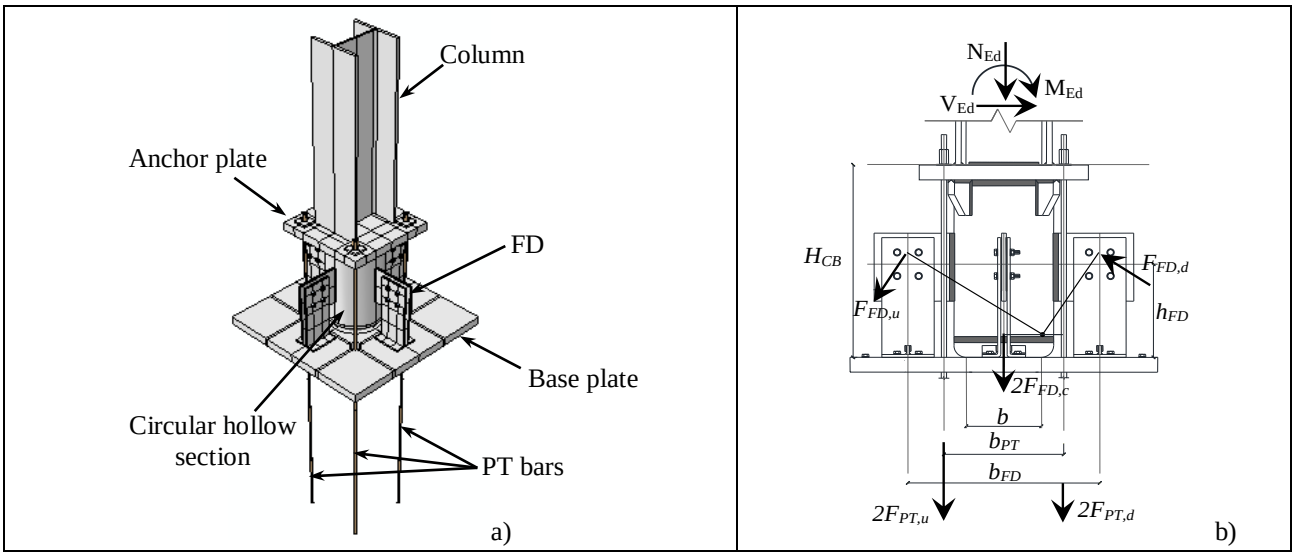

Fig. 1. a) 3D view of the proposed column base; b) fundamental dimensions and forces in the FDs and PT bars at the onset of rocking for loading from left to right

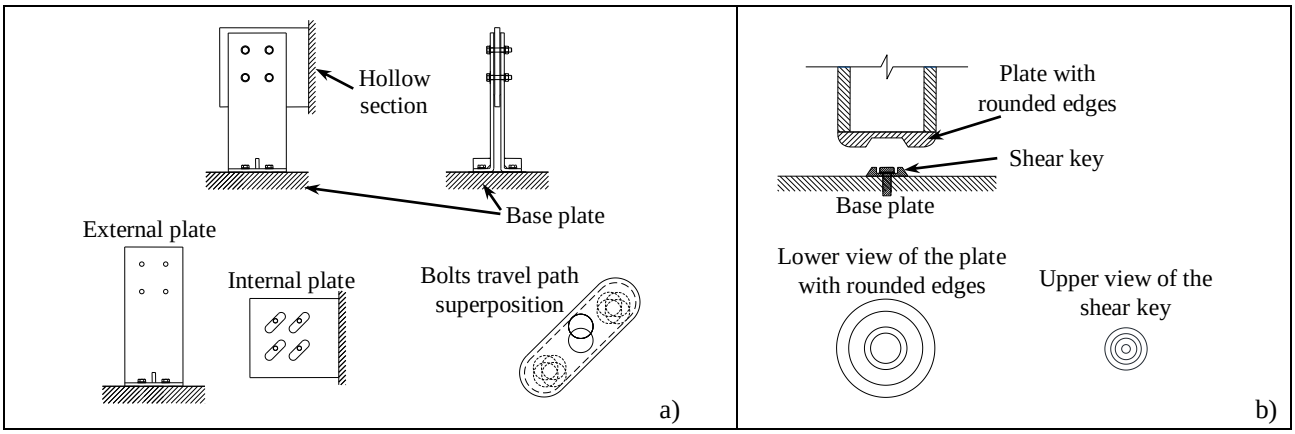

Fig. 2. a) Details of the friction device; b) steel plate with rounded edges and shear key

2.2 Moment-Rotation Behavior

Fig. 1(b) shows the fundamental dimensions of the column base that control the moment-rotation behavior in the rocking direction, *i.e. b* is the dimension of the contact surface; b_{PT} is the distance among the PT bars; b_{FD} is the distance among the centers of the FDs; and h_{FD} is the distance of the centers of the FDs from the base plate. *Fig. 1(b)* shows the forces in column base's components when it is at the onset of rocking with respect to its right edge under the effect of the internal axial force (N), shear force (V), and bending moment (M). In *Fig. 1(b)*, $F_{PT,u}$ and $F_{PT,d}$ are the forces in the PT bars, while $F_{FD,u}$, $F_{FD,d}$ and $F_{FD,c}$ are the forces in the FDs. The subscripts u and d denote whether the point of application of these forces will move upwards or downwards during rocking. The subscript c denotes the force in each of the two central FDs. The lever arms of the forces in the PT bars with respect to the center of rotation are given by:

$$z_{PT,u} = \left(b_{PT} + b\right)/2 \qquad z_{PT,d} = \left(b_{PT} - b\right)/2 \tag{1}$$

while the lever arms of the forces in the FDs are given by:

$$z_{FD,u} = \sqrt{\left[\left(b_{FD}+b\right)/2\right]^2 + h_{FD}^2} \qquad z_{FD,c} = b/2 \qquad z_{FD,d} = \sqrt{\left[\left(b_{FD}-b\right)/2\right]^2 + h_{FD}^2} \tag{2}$$

The moment contribution of the axial force, *N*, is given by:

$$M_N = N \cdot b/2 \tag{3}$$

The forces in each PT bar are function of the rotation, θ, of the column base and are given by:

$$F_{PT,u} = T_{PT} + K_{PT} \cdot z_{PT,u} \cdot \theta \qquad for \quad \theta \le \theta_{PT,u,y} \tag{4.a}$$

$$F_{PT,d} = T_{PT} - K_{PT} \cdot z_{PT,d} \cdot \theta \qquad for \quad \theta \le \theta_{PT,d,f} \tag{4.b}$$

where T_{PT} is the initial post-tensioning force of each PT bar; $K_{PT} = E_{PT}A_{PT}/L_{PT}$ is the stiffness of each PT bar; E_{PT}, A_{PT} and L_{PT} are respectively the Young's modulus, the cross-sectional area and the length of each PT bar; $\theta_{PT,u,y}$ is the rotation at which the PT bars (in position *u*) yield; and $\theta_{PT,d,f}$ is the rotation at which the force of the PT bars (in position *d*) becomes zero, *i.e.* when loss of post-tensioning occurs. The PT bars should be designed to avoid either yielding or loss of post-tensioning for a target rotation θ_T by using the following inequalities:

$$\theta_{PT,u,y} = \frac{F_{PT,y} - T_{PT}}{K_{PT} \cdot z_{PT,u}} \quad \rightarrow \quad L_{PT} \ge \frac{E_{PT} \cdot A_{PT} \cdot z_{PT,u} \cdot \theta_T}{F_{PT,y} - T_{PT}} \tag{5.a}$$

$$\theta_{PT,d,f} = \frac{T_{PT}}{K_{PT} \cdot z_{PT,d}} \quad \rightarrow \quad T_{PT} \ge K_{PT} \cdot z_{PT,d} \cdot \theta_T \tag{5.b}$$

where $F_{PT,y} = f_{y,PT} \cdot A_{PT}$ is the yield force of the PT bars and $f_{y,PT}$ is the yield stress of their steel material. Therefore, the moment contribution of the PT bars is given by:

$$M_{PT}(\theta) = 2\left[T_{PT}\left(z_{PT,u} - z_{PT,d}\right) + K_{PT}\left(z_{PT,u}^2 + z_{PT,d}^2\right)\theta\right] \qquad for \ \theta \le \theta_T \tag{6}$$

The friction force, $F_{FD,i}$, in each FD is given by:

$$F_{FD,i} = \mu_{FD} \cdot n_b \cdot N_b \qquad with \qquad i = u,c,d \tag{7}$$

where μ_{FD} is the friction coefficient of the surfaces in contact; n_b is the number of bolts and N_b is the bolt preloading force. Therefore, the moment contribution of the FDs is given by:

$$M_{FD} = 2 \cdot F_{FD}\left(z_{FD,u} + 2 \cdot z_{FD,c} + z_{FD,d}\right) \tag{8}$$

Fig. 3(a) shows the moment contributions of the axial force, M_N; the PT bars, M_{PT}; and the FDs, M_{FD}. The decompression moment, M_E, and the moment at the onset of rocking, M_D, are given by:

$$M_E = M_N + M_{PT,0} \tag{9}$$

$$M_D = M_E + M_{FD} \tag{10}$$

where $M_{PT,0}$ is the moment provided by the PT bars at zero rotation (*i.e.* $\theta=0.0$ in *Eq. (6)*).
The rotational stiffness contribution of the PT bars is given by:

$$S_{PT} = 2K_{PT}\left(z_{PT,u}^2 + z_{PT,d}^2\right) \tag{11}$$

and therefore, the moments corresponding to points 1 to 4 of the cyclic M-θ behavior of the column base in *Fig. 3(b)* are given by:

$$M_1 = M_D = M_N + M_{PT,0} + M_{FD} \tag{12.a}$$

$$M_2 = M_D + S_{PT}\theta_2 \tag{12.b}$$

$$M_3 = M_D + S_{PT}\theta_2 - 2M_{FD} \tag{12.c}$$

$$M_4 = M_D - 2M_{FD} \tag{12.d}$$

To ensure that the column base provides full self-centering capability, $M_4 \geq 0$ or $M_E \geq M_{FD}$.

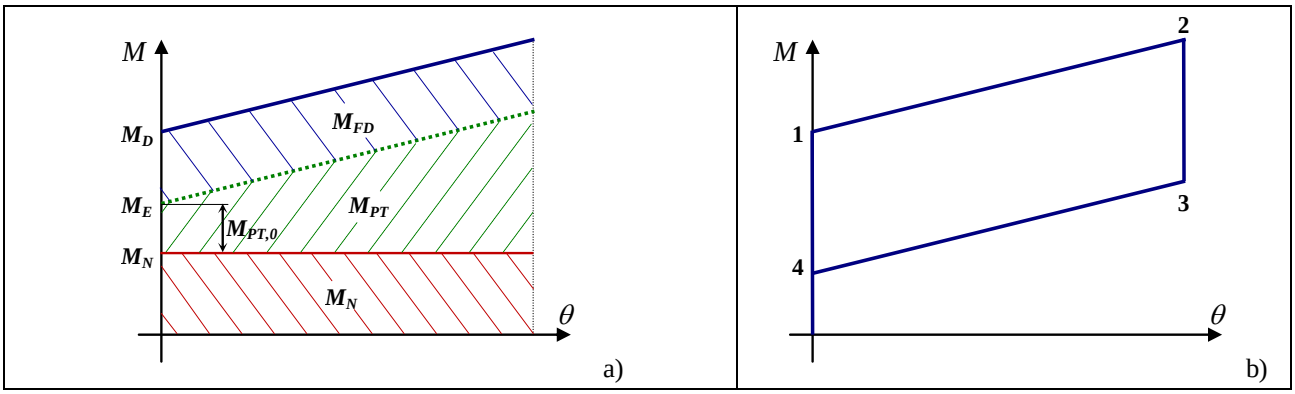

Fig. 3. Moment-rotation behavior of the column base. a) Moment contribution of the axial force, M_N; of the PT bars, M_{PT}; and of the FDs, M_{FD}; b) hysteretic behavior

The aforementioned equations do not account for geometrical, material and mechanical nonlinearities (*i.e.* P-Δ effects, PT bar yielding and loss of post-tensioning in the PT bars). Analytical equations accounting for such nonlinearities are provided in Freddi et al. [17]. The accuracy of the analytical equations has been evaluated by comparison with the results of ABAQUS simulations [17].

3 DESIGN PROCEDURE FOR THE ROCKING COLUMN BASE

This section describes the steps of a design procedure that ensures that the column base has damage-free behavior, self-centering capability, and adequate energy dissipation capacity. The design procedure requires as input the cross-section of the column; the axial force in the column due to the gravity loads of the seismic load combination, $N_{Ed,G}$; the axial force due to the seismic load combination, N_{Ed}; and the 1st story drift due to the seismic load combination.

3.1 Design Procedure

The fundamental dimensions of the column base (*i.e.* b, b_{PT}, b_{FD}, and h_{FD}) which define the parameters $z_{PT,u}$, $z_{PT,d}$, $z_{FD,u}$, $z_{FD,c}$ and $z_{FD,d}$ are selected by practical and geometric considerations.

The moment at the target rotation, M_T, should be lower than the plastic moment of resistance of the column, $M_{N,Rd}$, to protect the latter from yielding. Therefore, M_T is defined as $M_T = M_{N,Rd}/\gamma_T$ where γ_T can be calculated as $1.1\gamma_{ov}$ according to Eurocode 8 [1] where the material over-strength factor, γ_{ov} can be assumed equal to 1.25. Therefore, the typical value of γ_T is 1.375. On the other hand, to ensure self-centering behavior, the moment provided by the FDs, M_{FD}, should not exceed the decompression moment, M_E. Therefore, M_E is defined as $M_{FD} = M_E/\alpha_{sc}$ where α_{sc} is a design parameter with a value larger than unity. Recommendations for the choice of appropriate values for the parameter α_{sc} is out of the scope of the present paper and will be a task after a near future experimental evaluation of the column base.

By defining $\kappa = \sigma_{PT}/f_{y,PT}$ as the stress ratio in the PT bars (σ_{PT} as the stress in the PT bars), the moment at the target rotation, M_T, can be calculated as:

$$M_T = M_E + M_{FD} + S_{PT}\theta_T = \left(1+\frac{1}{\alpha_{sc}}\right)\left[N_{Ed}\frac{b}{2} + 2\kappa A_{PT} f_{y,PT}\left(z_{PT,u} - z_{PT,d}\right)\right] + 2\frac{E_{PT}A_{PT}}{L_{PT}}\left(z_{PT,u}^2 + z_{PT,d}^2\right)\theta_T \tag{13}$$

Further re-arrangement of *Eq. (13)* provides:

$$\kappa = \frac{1}{2A_{PT} f_{y,PT}\left(z_{PT,u} - z_{PT,d}\right)}\left[\left(M_T - 2\frac{E_{PT}A_{PT}}{L_{PT}}\left(z_{PT,u}^2 + z_{PT,d}^2\right)\theta_T\right) \Big/ \left(1+\frac{1}{\alpha_{sc}}\right) - N_{Ed}\frac{b}{2}\right] \tag{14}$$

Eq. (14) shows that κ, A_{PT} and L_{PT} are the design variables, while all the other parameters are selected by the designer. A simple re-arrangement of *Eq.s (5)* yields:

$$\kappa \le 1 - \frac{E_{PT} \cdot z_{PT,u} \cdot \theta_T}{f_{y,PT} \cdot L_{PT}} = \kappa_{\max} \tag{15.a}$$

$$\kappa \ge \frac{E_{PT} \cdot z_{PT,d} \cdot \theta_T}{f_{y,PT} \cdot L_{PT}} = \kappa_{\min} \tag{15.b}$$

Eq. (14) together with *Eq.s (5)* can be used to calculate the design variables of the problem as reported in the following example.

3.2 Design Example

On the basis of a realistic building design case, the novel column base is designed for a HEB 300 column cross-section; axial force $N_{Ed,G}$ equal to 537.8kN; and axial force N_{Ed} equal to 565.3kN. The plastic moment of resistance $M_{N,Rd}$ is calculated equal to 308.9kNm. The target rotation is assumed equal to 0.023rads. Based on the geometry of the column cross-section, a circular hollow section with 323.9mm diameter and 40mm thickness is adopted. A circular steel plate with the same diameter is welded at the bottom of the hollow section. Standard mechanical processing provides this plate with rounded circular edges having a radius of 40mm as well as with appropriate space to accommodate the shear key. The contact surface has a dimension b equal to 243.9mm. The anchor plate of the PT bars in the top of the hollow steel section is square and has width and thickness equal to 550mm and 50mm, respectively. The distance among the PT bars b_{PT} is selected equal to 390.0mm. The PT bars materials properties are E_{PT} = 205GPa and $f_{y,PT}$ = 900MPa.

Fig. 4(a) shows the variation of κ with respect to L_{PT} for different d_{PT} values. The coefficients γ_T and α_{sc} have been assumed equal to 1.4 and 1.3, respectively. Any pair of κ and L_{PT} with values within the highlighted acceptable zone can be selected. However, the optimum design that satisfies the design criteria and minimizes the length of the PT bars should be a point close to the intersection of the $\kappa_{\min}$ and $\kappa_{\max}$ curves. In this example, d_{PT} is selected equal to 15mm, L_{PT} equal to 2240mm, and κ equal to 0.189. The latter corresponds to T_{PT} equal to 30.0kN. The rotations $\theta_{PT,u,y}$ and $\theta_{PT,d,f}$ are equal to 0.0252rads and 0.0255rads, respectively. *Fig. 4(b)* shows the moment-rotation behavior for the column base. The decompression moment, M_E, the moment at the onset of rocking, M_D, and the moment provided by the FDs, M_{FD}, are equal to 80.3kNm, 142.0kNm and 61.7kNm, respectively.

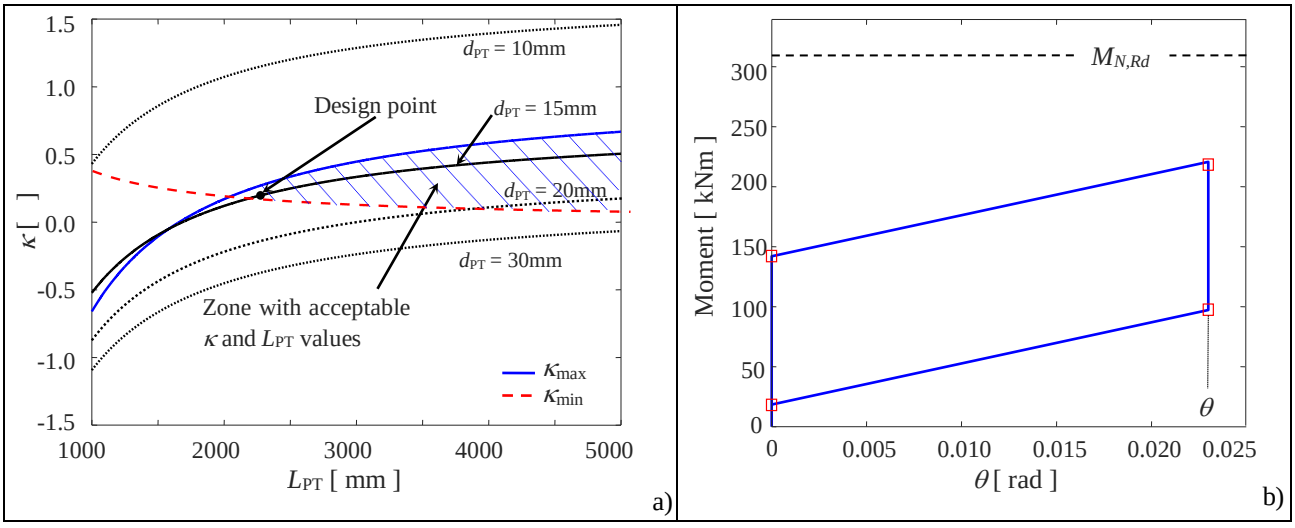

Fig. 4. a) Variation of κ with respect to L_{PT} for different d_{PT} values; (b) moment-rotation behavior of the column base

FDs are introduced on the four sides of the column base; the relevant dimensions are b_{FD} = 623.9mm and h_{FD} = 315mm. The friction coefficient at the brass-steel interface is assumed equal to 0.15. M12 class 10.9 bolts are preloaded at 45kN by tightening.

4 EFFECT OF ROCKING COLUMN BASE ON GLOBAL SEISMIC RESPONSE

4.1 OpenSees Nonlinear Model for the Column Base

A simplified two-dimensional nonlinear model in OpenSees [16] is developed to simulate the cyclic behavior of the proposed column base. The OpenSees model is shown in *Fig. 5*. 'Elastic beam-column' elements with very high flexural stiffness are used to model the almost rigid components of the column base, *i.e.* the interface where rocking takes place; the anchor plate and the internal plates of the FDs.

To capture rocking behavior, 'zero-length' contact spring elements associated with the 'elastic compression-no tension' material of OpenSees [16] are used to connect the nodes of the column base and the fixed nodes of the column base at the locations of the centers of rotation. The compression stiffness of the contact springs is assumed equal to 20 times the axial stiffness of the column following the modeling approach in [20]. Larger values of this stiffness were found to produce practically the same results but with higher computational cost.

PT bars are modeled using truss elements running parallel to the column center-line axis and connected to the rigid elements simulating the anchor plate. To simulate loss of post-tensioning, a 'zero-length' contact spring with an 'elastic compression-no tension' material is introduced between the PT bars and the anchor plate. The truss elements have a cross-section area equal to the area of two PT bars to simulate the four PT bars of the column base in a simple way. To account for post-tensioning, an initial strain equal to $F_{PT,i}/(A_{PT}E_{PT})$ is first assigned to the truss element. Post-tensioning results in shortening of the circular hollow section, which in turn decreases the post-tensioning force. To account for this decrease, the initial strain in the 'truss' element was increased to ensure that the post-tensioning force in the PT bars will be equal to $F_{PT,i}$ after the hollow section shortening. The 'InitStrainMaterial' [16] along with the elastoplastic material 'Steel01' is used for the PT bars truss elements.

The FDs are modeled by using truss elements placed at appropriate locations in order to account for their true level arms. A bilinear elastic-plastic material ('Steel 01' material in OpenSees [16]) with very high initial stiffness and very low post-elastic stiffness is assigned to these truss elements in order to model the FDs behavior. The yield stress assigned to the material model and the area of the truss elements are appropriately defined to represent the friction force in the FDs. The OpenSees model has been validated against the results of the ABAQUS FE model developed by Freddi et al. [17].

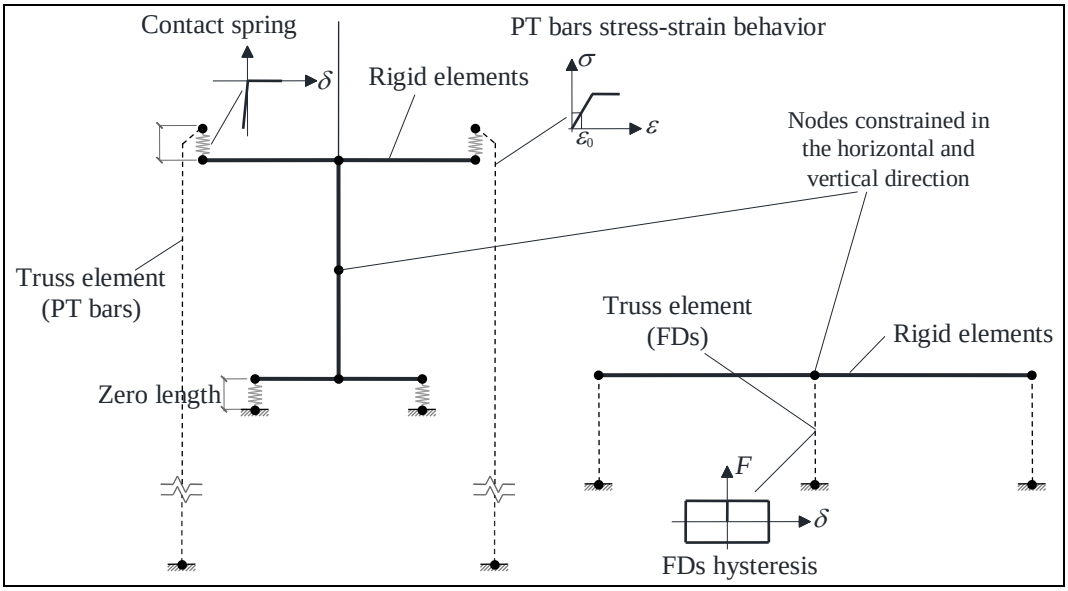

Fig. 5. OpenSees model for the column base

4.2 Seismic Design

Fig. 6 shows the plan and elevation views of a 5-story, 5-bay by 3-bay prototype steel building having two identical perimeter seismic-resistant frames in the *x* plan direction. The study focuses on

one perimeter seismic-resistant frame. This frame is designed as a SC-MRF using PT beam-column connections with the aid of the design procedure proposed in [21]. The interior gravity frames (with pinned beam–column connections and pinned column bases) are coupled with the SC-MRF through the floor diaphragm.

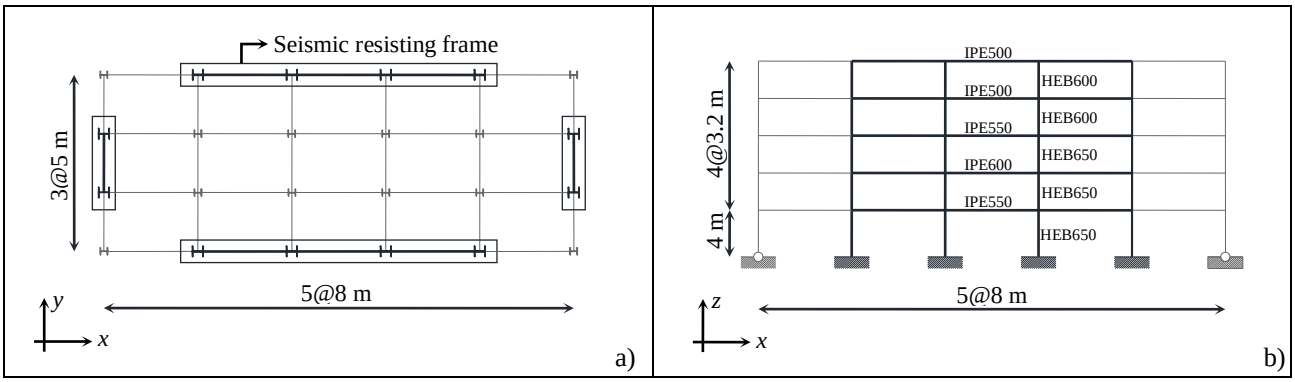

Fig. 6. a) Plan view; b) elevation view of the prototype building and dimensions of structural elements of the SC-MRF

The building is designed assuming the target story drift ($\theta_{s,max}$) under the frequently occurred earthquake (probability of exceedance of 10% in 10yrs) equal to 0.75% [1]. The design basis earthquake (DBE; probability of exceedance of 10% in 50yrs) is expressed by the Type 1 elastic response spectrum of Eurocode 8 [1] with peak ground acceleration equal to 0.35g and ground type B. The maximum credible earthquake (MCE) is assumed to have intensity equal to 150% the DBE intensity. The model used for the design is based on centerline dimensions without accounting for the finite panel zone dimensions. The steel yield strength is equal to 355MPa for the columns, 275MPa for beams and 900MPa for PT bars. The design results in the beam and column cross-sections provided in *Fig. 6(b)*. The SC-MRF is designed with rigid full-strength conventional column bases. For the same SC-MRF design, rocking damage-free column bases are also designed.

4.3 Models for the SC-MRFs and Earthquake Ground Motions

FE models for the SC-MRFs are developed in OpenSees [16]. The models use fiber beam-column elements for the beams and columns, while appropriate combinations of zero-length nonlinear rotational springs are used for the panel zones, the PT beam-column connections, and the locations where beam plastic hinges are expected. More information on modeling SC-MRFs in OpenSees can be found in [20]. The rocking column bases are modeled as described in Section 4.1. The SC-MRF with conventional column bases has T_1 equal to 0.94sec, while the SC-MRF with the rocking column bases has T_1 equal to 0.867sec. The latter difference is due to the shorter flexible length of the first story columns of the SC-MRF with the rocking column bases. Ten earthquake ground motions (selected from the far-fault ground motions developed by the FEMA P694 project [22]) are used for nonlinear dynamic analyses. They are scaled to the DBE and MCE seismic intensities which is described by the spectral acceleration, S_a, at T_1, while the inherent damping ratio is 3%.

4.4 Seismic Analyses Results

The analyses results, highlight that in terms of peak story drifts of the SC-MRFs the use of the rocking column base results in modest increase of the 1st story drift and modest decrease of the drifts of the upper stories. In terms of residual story drifts it is observed that the SC-MRF with conventional column bases experiences appreciable residual 1st story drifts due to 1st story column yielding. Such residual drifts reach values close to 0.5% under individual earthquake ground motions (*i.e.* a critical value that is considered as the limit beyond which repair of a steel building may not be economically viable [20]). On the other hand, the use of the rocking column base essentially eliminates the 1st story residual drift.

Fig. 7(a) shows the 1st story drift time histories of the SC-MRFs for a specific earthquake ground motion scaled at the DBE intensity. This figure highlights that the two SC-MRFs experience similar peak 1st story drifts but the residual 1st story drifts are minimized for the SC-MRF with the rocking column bases. For the same earthquake ground motion, *Fig. 7(b)* compares the stress-strain

hysteresis in the flanges of one of the 1st story columns of the SC-MRFs. These figures show that the SC-MRF with conventional column bases experience plastic deformations and damage that needs to be repaired in the aftermath of strong earthquakes, while the SC-MRF with rocking column bases fully protects the columns from yielding under both the DBE and MCE.

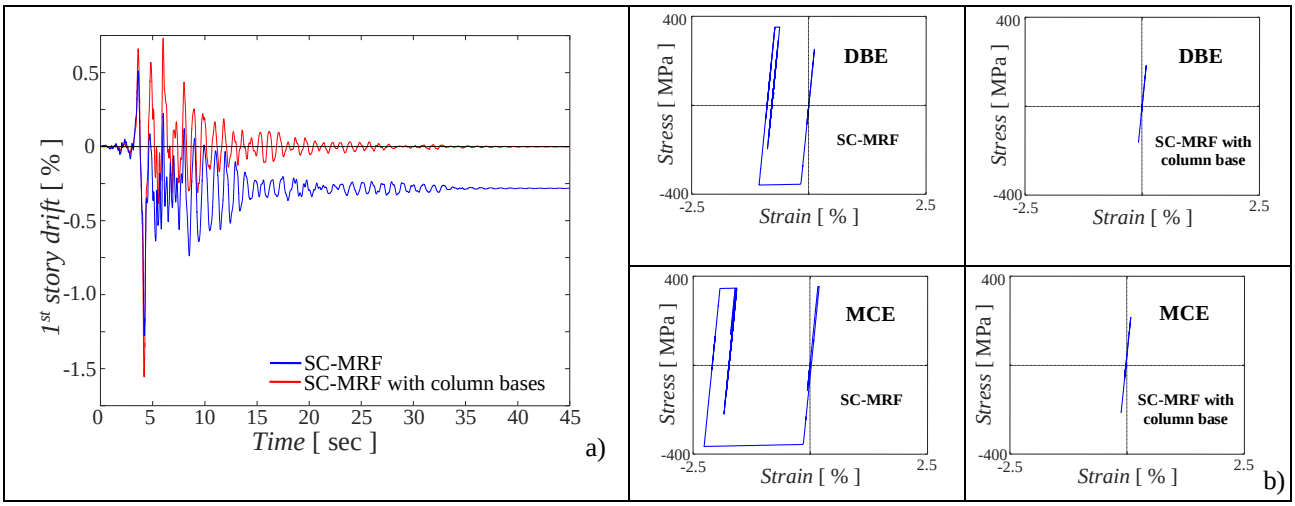

Fig. 7. a) 1st story drift time histories for a specific ground motion scaled at the DBE intensity; (b)Stress-strain hysteresis in the flanges of one of the 1st story columns of the SC-MRFs for a specific ground motion scaled at the DBE and MCE intensities

5 CONCLUSIONS

A rocking damage-free steel column base has been presented. The column base uses post-tensioned (PT) high strength steel bars to control rocking behavior and friction devices to dissipate seismic energy. Contrary to conventional steel column bases, the rocking column base has monotonic and cyclic moment-rotation behaviors that are easily described using simple analytical equations. Analytical equations are provided for different cases including structural limit states that involve yielding or loss of post-tensioning in the PT bars. A step-by-step design procedure was presented, which ensures damage-free behavior, self-centering capability, and adequate energy dissipation capacity under a predefined target column base rotation. The procedure provides optimum designs of the column base by using a simple graphical method. A three-dimensional non-linear finite element (FE) model of the column base was developed in ABAQUS by Freddi et al. [17]. The results of the FE simulations validate the accuracy of the moment-rotation analytical equations and demonstrate the efficiency of the design procedure. A simplified model for the column base was developed in OpenSees and validated against the detailed FE models [17]. A prototype steel building was designed as a self-centering moment-resisting frame with conventional or rocking column bases. Nonlinear dynamic analyses show that the rocking column base fully protects the 1st story columns from yielding and eliminate the 1st story residual drift without any detrimental effect on peak story drifts.

6 ACKNOWLEDGMENT

This research is supported by Marie Sklodowska-Curie Action Fellowships within the H2020 European Programme. Any opinions, findings, and conclusions or recommendations expressed in this paper are those of the authors and do not necessarily reflect the views of the European Commission.

REFERENCES

[1] Eurocode 8. “Design of structures for earthquake resistance. Part 1: General rules, seismic action and rules for buildings”. *European Committee for Standardization*, Brussels, Belgium, 2005.

[2] Federal Emergency Management Agency. FEMA 350. “Recommended seismic design criteria for new steel moment-frame buildings”. *SAC Joint Venture*, Washington, DC, 2000.

[3] Christopoulos C., Filiatrault A. “Principles of passive supplemental damping and seismic isolation”. *IUSS Press*, Pavia, Italy, 2006.

[4] Chancellor N.B., Eatherton M.R., Roke D.A., Akbas T. “Self-centering seismic lateral force resisting systems: High-performance structures for the city of tomorrow”. *Buildings*, No. 4, pp. 520-548, 2014.

[5] Eurocode 3. “Design of steel structures – Part 1.8: Design of Joints”. *European Committee for Standardization*, Brussels, Belgium, 2005.

[6] Latour M., Rizzano G. “Full strength design of column base connections accounting for random material variability”. *Engineering Structures*, No. 48, pp. 458-471, 2013.

[7] Latour M., Rizzano G. “A theoretical model for predicting the rotational capacity of steel base joints”. *Engineering Structures*, No. 91, pp. 89-99, 2013.

[8] Kanvinde A.M., Grilli D.A., Zareian F. “Rotational stiffness of exposed column base connections: experiments and analytical models”. *Journal of Structural Engineering* (ASCE), No. 138(5), pp. 549-560, 2012.

[9] Grauvilardell J.E., Lee D., Hajjar J.F., Dexter R.J. “Synthesis of design, testing and analysis research on steel column base plate connections in high-seismic zones”. Report ST-04-02, Dept. of Civil Engineering, Univ. of Minnesota, USA, 2006.

[10] Mackinven H., MacRae G.A., Pampanin S., Clifton G.C., Butterworth J. “Generation four steel moment frame joints”. Proceedings of the 8th Pacific Conference on Earthquake Engineering, Singapore, 2007.

[11] MacRae G.A., Urmson C.R., Walpole W.R., Moss P., Hyde K., Clifton C. “Axial shortening of steel columns in buildings subjected to earthquakes”. *Bulletin of the New Zealand Society for Earthquake Engineering*, No. 42(4), pp. 275–287, 2009.

[12] Yamanishi T., Kasai K., Takamatsu T., Tamai H. “Innovative column-base details capable of tuning rigidity and strength for low to medium-rise steel structures”. Proceedings of the 15th World Conference on Earthquake Engineering, Lisbon, Portugal, 2012.

[13] Chi H., Liu J. “Seismic behavior of post-tensioned column base for steel self-centering moment resisting frame”. *Journal of Constructional Steel Research*, No. 78, pp. 117–130, 2012.

[14] Chou C-C., Chen J.H. “Analytical model validation and influence of column bases for seismic responses of steel post-tensioned self-centering MRF systems”. *Engineering Structures*, No. 33(9), pp. 2628–2643, 2011.

[15] Borzouie J., MacRae G.A., Chase J.G., Rodgers G.W., Clifton G.C. “Experimental studies on cyclic performance of column base strong axis – aligned asymmetric friction connections”. *Journal of Structural Engineering* (ASCE), No. 142(1), 04015078, 2016.

[16] McKenna F., Fenves G.L., Scott M.H. “OpenSees: Open system for earthquake engineering simulation”. *PEER Center, Berkeley*, CA, 2006.

[17] Freddi F., Dimopoulos A.C., Karavasilis T.L. “Rocking damage-free steel column base with friction devices: design procedure and numerical evaluation”, *Earthquake Engineering & Structural Dynamics, in Press.*

[18] ABAQUS/Standard and ABAQUS/Explicit – Version 6.13.1. ABAQUS Theory Manual, Dassault Systems, 2013.

[19] Kamperidis V.C., Karavasilis T.L., Vasdravellis G. “Design and modeling of a novel damage-free steel column base”. Proceedings of the 8th International Conference on Advances in Steel Structures. Lisbon, Portugal, 2015.

[20] Dimopoulos A.I., Tzimas A.S., Karavasilis T.L., Vamvatsikos D. “Probabilistic economic seismic loss estimation in steel buildings using post-tensioned moment-resisting frames and viscous dampers”. *Earthquake Engineering & Structural Dynamics*, DOI: 10.1002/eqe.2722, 2016.

[21] Tzimas A.S., Dimopoulos A.I., Karavasilis T.L. “EC8-based seismic design and assessment of self-centering post-tensioned steel frames with viscous dampers”. *Journal of Constructional Steel Research*, No. 105, pp. 60–73, 2015.

[22] FEMA P695. “Quantification of building seismic performance factors”. ATC-63 Project. *Applied Technology Council*, CA, USA, 2008.